FIRST EVIDENCE OF PROTEIN MODULATION BY POLYSTYRENE MICROPLASTICS IN A FRESHWATER BIOLOGICAL MODEL

Magni[a], S., Della Torre[a], C., Garrone[b], G., D'Amato[c], A., Parenti[a], C.C., Binelli[a*], A.

[a]Department of Biosciences, University of Milan, Via Celoria 26, 20133 Milan, Italy

[b]UNITECH OMICS Platform, University of Milan, Viale Ortles 22/4, 20139 Milan, Italy

[c]Department of Pharmaceutical Sciences (DISFARM), University of Milan, Via Mangiagalli 25, 20133 Milan, Italy

ABSTRACT

Microplastics (MPs) are now one of the major environmental problems due to the large amount released in aquatic and terrestrial ecosystems, as well as their diffuse sources and potential impacts on organisms and human health. Still the molecular and cellular targets of microplastics' toxicity have not yet been identified and their mechanism of actions in aquatic organisms are largely unknown. In order to partially fill this gap, we used a mass spectrometry based functional proteomics to evaluate the modulation of protein profiling in zebra mussel (*Dreissena polymorpha*), one of the most useful freshwater biological model. Mussels were exposed for 6 days in static conditions to two different microplastic mixtures, composed by two types of virgin polystyrene microbeads (size=1 and 10 μm) each one. The mixture at the lowest concentration contained 5×10^5 MPs/L of 1μm and 5×10^5 MPs/L of 10 μm, while the higher one was arranged with 2×10^6 MPs/L of 1 μm and 2×10^6 MPs/L of 10 μm.

Proteomics' analyses of gills showed the complete lack of proteins' modulation after the exposure to the low-concentrated mixture, while even 78 proteins were differentially modulated after the exposure to the high-concentrated one, suggesting the presence of an effect-threshold. The modulated proteins belong to 5 different classes mainly involved in the structure and function of ribosomes, energy metabolism, cellular trafficking, RNA-binding and cytoskeleton, all related to the response against the oxidative stress.

Capsule: a mixture of polystyrene microplastics (2×10^6 MPs/L of 1 μm and 2×10^6 MPs/L of 10 μm) was able to modulate 78 different proteins of the zebra mussels' gills most involved in the oxidative stress response.

*Corresponding Author: Andrea Binelli (andrea.binelli@unimi.it), Department of Biosciences, University of Milan, Via Celoria 26, 20133 Milan (Italy)

HIGHLIGHTS

1) Effect of polystyrene microplastics on protein regulation of a freshwater organism
2) The highest microplastic concentration modulated 78 different proteins
3) The most modulated proteins are involved in the response against oxidative stress

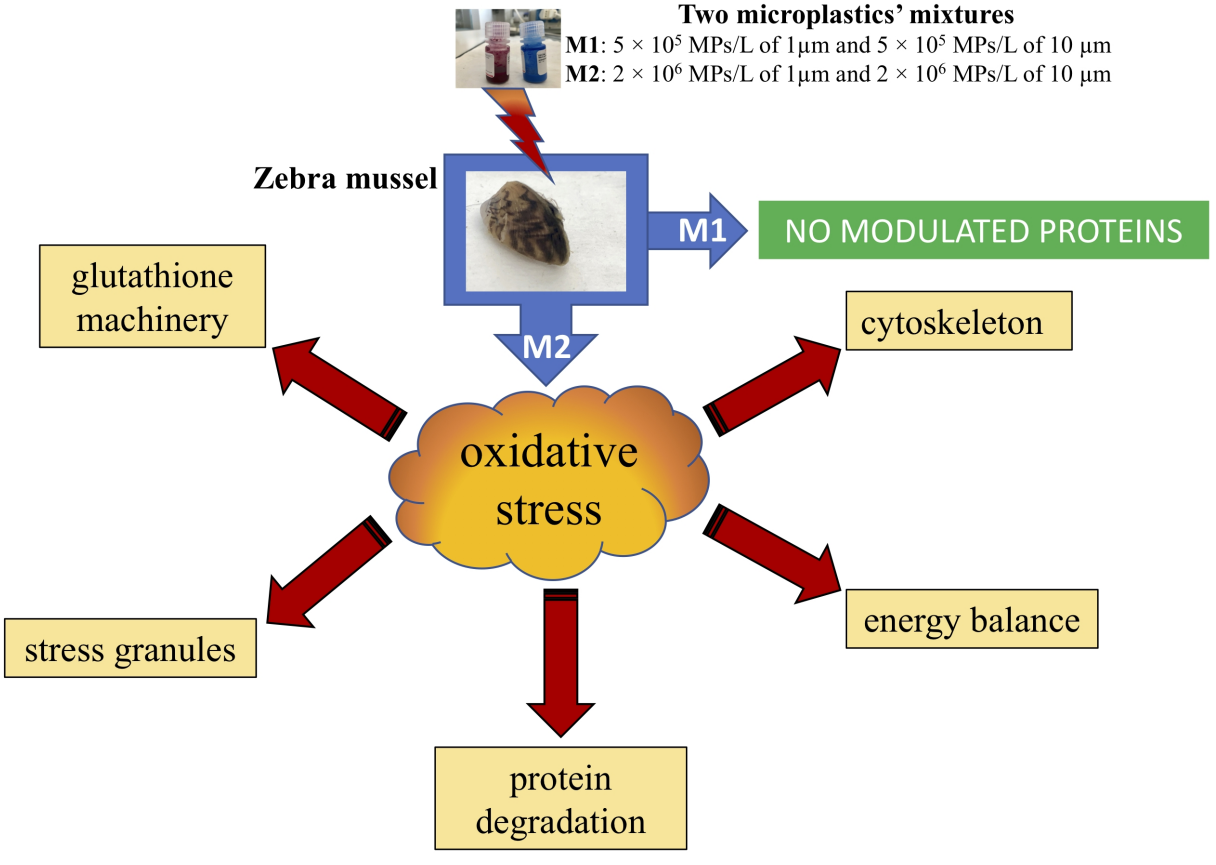
Two microplastics' mixtures
M1: 5 × 10^5 MPs/L of 1µm and 5 × 10^5 MPs/L of 10 µm
M2: 2 × 10^6 MPs/L of 1µm and 2 × 10^6 MPs/L of 10 µm
Zebra mussel
M1
NO MODULATED PROTEINS
M2
glutathione machinery
cytoskeleton
oxidative stress
stress granules
energy balance
protein degradation

INTRODUCTION

The increasing production and use of plastic goods and mainly their improper disposal, as well as the poor management of plastic wastes, have led to a great and continuous release of plastics in terrestrial and water ecosystems. Plastics are now one of the main challenges in the environmental management since the solution or more probably the mitigation of this problem affects the lifestyle, habits and behavior of each of us. In the last years, the scientific community focused the attention to microplastics (MPs), which are recently re-defined as synthetic polymers from 1 to <1000 μm in the largest dimension (Hartmann et al., 2019). They derive from two different sources: the primary MPs originate from some plastic products, such as toothpastes, scrubs, cosmetics or pellets used in plastic production (Hidalgo-Ruz et al., 2012; Carr et al., 2016), while secondary MPs are small debris degraded through physical, chemical and biological processes from large plastics, such as shopping bags, fishing nets, resin pellets and household items (Browne et al., 2007). Although the MPs from terrestrial sources contribute to 80% of the total plastic debris that reach marine ecosystems (Cole et al., 2011), only few studies were conducted in freshwaters, as recently highlighted by Lambert and Wagner (2018) who indicated that less than 4% of studies related to MPs can be associated to inland waters. The MPs in freshwaters are characterized by an outstanding heterogeneity depending on sampling location, weather conditions, human activities and also sampling approaches (Eerkes-Medrano et al., 2015). The mean density of MPs in freshwaters changes dramatically, varying from almost none to many million MPs/m^3 (Li et al., 2018). The environmental impact of MPs can be categorized to physical, chemical and toxicological effects, each of them were identified mainly in marine organisms.

While the physical impacts of macroplastics include entanglement and ingestion which cause drowning, suffocation, strangulation and starving (Allsopp et al., 2006), MPs' ingestion can damage the gastrointestinal tract by mechanical rubbing and physical blockage of digestive organs (Jovanovic, 2017). The chemical and toxicological impacts are linked both to the intrinsic toxicity of MPs, but especially to the effects of additives, such as phthalates and bisphenol A used as plasticizers (Hammer et al., 2012), or to the plethora of environmental pollutants adsorbed on their surface that can be firstly ingested with MPs and then released in the organism even faster than that in the environment (Bakir et al., 2014). Up to now, only few studies were carried out in freshwater organisms: a very recent research showed an inhibition of cholinesterase activity on the bivalve *Corbicula fluminea* due to a mixture of the antimicrobial florfenicol and MPs (Guilhermino et al., 2018), while several studies conducted on larval and adult zebrafish (*Danio rerio*) demonstrated as MPs caused locomotion alteration, intestinal damage and metabolic changes (Lu et al., 2016; Chen et al., 2017; Sleight et al., 2017; Lei et al., 2018). Ding and collaborators (2018) found an activation

of EROD (7-ethoxyresorufin O-deethylase), BFCOD (7-benzyloxy-4-trifluoromethyl-coumarin O-dibenzyloxylase) and SOD (superoxide dismutase) in the liver, as well as an inhibition of AChE (acetylcholinesterase) in the brain of the fish red Tilapia (*Oreochromis niloticus*) exposed for 14 days to 0.1 mm polystyrene MPs administered at different concentrations. Instead, Weber and co-workers (2018) have not monitored any significant effects on survival, development, metabolism and feeding activity in the freshwater crustacean *Gammarus pulex* exposed to irregular fragments of polyethylene terephthalate (PET; 10-150 μm) for 48 h. Our previous results obtained on the same freshwater zebra mussel (*Dreissena polymorpha*) used in this proteomic study showed a significant ($p<0.05$) increase of catalase and dopamine and a significant ($p<0.05$) decrease of glutathione peroxidase (Magni et al., 2018).

Therefore, in order to partially fill this gap of knowledge on the impact of MPs in freshwater organisms, we investigated the possible proteins' modulation in zebra mussels (*Dreissena polymorpha*) exposed to two different concentrations of a mixture of two types of virgin polystyrene microbeads (size=1 and 10 μm). We carried out static exposures for 6 days, performing proteomics analyses on mussels' gills, considering that this organ can represent a route of entrance for these emerging contaminants and that gills could be a target for MPs, being the first barrier that they encounter when enter through the inhalant siphon of mussels. The selection of zebra mussel as biological model is due to its specific characteristics, such as high filtration rate, easiness in laboratory maintenance, size suitable to expose a significant number of specimens and its ecological position that links littoral and benthic ecosystems (Binelli et al., 2015). Mass spectrometry-based proteomics is one of the most sensitive methodology available in ecotoxicology (Monsinjon and Knigge, 2007) and allowed us to study the potential toxicity of the virgin MPs. To our knowledge, this represents the first attempt to investigate the possible role played by MPs to modulate the proteins' expression of a freshwater organism.

2. MATERIALS AND METHODS

2.1 *Selection of concentrations and exposure to polystyrene MPs*

We collected hundreds of zebra mussels in Lake Iseo (Northern Italy) at 2-3 m of depth, then transported in lake water to the laboratory. Before the exposure tests, mussels were acclimated for 2 weeks in 15 L tanks (50:50 v/v of tap and deionized water), at 20 ± 1 °C under oxygen saturation and natural photoperiod, and fed with *Spirulina sp.*, as described in other previous studies (Binelli et al., 2015; Magni et al., 2016, 2017, 2018).

We purchased the standard suspension (5%) of polystyrene MPs (1 and 10 μm) from Sigma Aldrich (Milan, Italy), which were subsequently diluted in ultrapure water to reach 50 mg/L of suspensions.

Then, we quantified the number of the two types of MPs by a Bürker chamber, achieving $116 \times 10^6 \pm 33 \times 10^6$ of 10 μm MPs/L and $23 \times 10^9 \pm 530 \times 10^6$ of 1 μm MPs/L, respectively. We did not notice any MPs' aggregation in the working suspensions observed by confocal microscopy (Magni et al., 2018). We measured the number of MPs only in the working suspensions, because it was impossible their measurement in the exposure beakers. We tried by coulter counter, but the lack of any surface charge prevents any possible realistic measure. Then, we tried by the Bürker chamber, by which we measured the MPs in the working suspensions. However, after the dilutions to reach the selected concentration in the exposure beakers, the average number of 10 μm microparticles in M2 (the highest suspension) was only 1.8 particles in the Bürker chamber: 2.000.000 particles/L = 2 particles/μL (mm^3). Then, (2 particles/mm^3) x 9 mm^2 (chamber area) = 18 particles/mm x 0.1 mm (thickness of chamber) = 1.8 average total particles in the Bürker chamber. This low value made not possible a plausible evaluation of the final suspensions' concentration. Furthermore, MPs of 1 μm were impossible to check in the exposure beakers due to their small size and the presence of the microalgae used as food that interfere on the microscopy observations.

Since the aim of this study was the preliminary investigation of the possible role of this kind of MPs to modulate the proteome of a non-target freshwater organism, we selected two MPs' concentrations higher than those now found in the inland waters in order to evaluate the mechanism of action (MoA) of these physical environmental contaminants. The reason is exactly the same even for the choice to use two mixtures of MPs with two different sizes (1 and 10 μm): the first one (M1) with 5×10^5 MPs/L of 1μm and 5×10^5 MPs/L of 10 μm (total amount: 1×10^6 MPs/L), while the second one (M2) with 2×10^6 MPs/L of 1μm and 2×10^6 MPs/L of 10 μm (total concentration: 4×10^6 MPs/L).

Exposures were carried out in triplicate (3 tanks for controls, M1 and M2, respectively), placing 70 mussels on suspended nets in each 4L glass beakers (n=9) for each of the two mixtures (Ms) and related control for 6 days in static conditions in the same maintenance conditions above mentioned and under slow stirring to prevent the MPs' sedimentation. Thus, the sample size for each treatment and controls was 210 each one (70 mussels/tank x 3 tanks) which were then used both for biomarker analyses and proteomics. The short exposure time is related to the onset of deleterious effects caused by the bivalve metabolism and the food degradation after 6 days due to the lack of water change.

We added food only two times during the exposure to avoid a possible effect simply due to the under-nutrition, but at the same time to eliminate any possible interference of algae to the MPs' bioavailability, bearing in mind that the aim of the study was the investigation of the potential toxicity of the only MPs. On the other hand, the primary effect of toxicants should appear early,

since it affects the molecular level at first. Indeed, we previously evaluated that this exposure time is sufficient to produce some cyto- and genotoxic effects, as well as proteins' modulation on this biological model (Binelli et al., 2015; Magni et al., 2018).

At the end of exposure, we dissected one gill from 5 mussels *per* treatment, randomly selected from the three beakers, then stored at -80 °C, while the other mussels were used for biomarkers measurements (Magni et al., 2018). Contemporarily, the other fresh dissected gill was quickly observed with an optical microscope without any preliminary treatment to confirm the presence of MPs in this tissue.

2.2 *Mass spectrometry based proteomic analysis*

2.2.1 Sample preparation

We homogenized a pool of 5 gills *per* treatment (1 gill for each mussel randomly selected from the three tanks) in 500 µL of lysis buffer containing 20 mM 4-(2-hydroxyethyl)-1-piperazineethanesulfonic acid pH = 7.5 (HEPES), 320 mM sucrose, 1 mM ethylenediaminetetraacetic acid pH = 8.5 (EDTA), 5 mM ethylene glycol-bis(β-aminoethyl ether)-N,N,N',N'-tetraacetic acid pH = 8.1 (EGTA), 1 mM sodium ortho-vanadate (Na_3VO_4), 10 mM β-glycerophosphate, 10 mM sodium fluoride (NaF), 10 mM sodium pyrophosphate (NaPPi), 1 mM phenylmethylsulfonyl fluoride (PMSF) in ethanol, 5 mM dithiothreitol (DTT) and protease inhibitors (Roche) in Milli Q® water (Binelli et al., 2017). We centrifuged the homogenates at 15,000 g (S15 fraction) for 10 min at 4 °C and quantified the proteins with Bradford method (Bradford, 1976); 300 µg of proteins were then precipitated with methanol/chloroform/Milli Q water (4:1:3 ratio v/v). Obtained pellets were re-suspended in 8 M urea in 50 mM tris hydrochloride (Tris-HCl), 30 mM sodium chloride (NaCl) pH = 8.5 and protease inhibitors (Roche) and centrifuged at 14,000 g for 30 min at 4 °C. We re-quantified the proteins in the supernatant with Bradford method (Bradford, 1976). Then, 10 µg of proteins were incubated with 50 mM DTT in 50 mM ammonium bicarbonate (AMBIC) for 30 min at 52 °C under stirring (600 rpm) to perform the reduction of disulfide bonds; subsequently, we added in each sample 100 mM iodoacetamide ($IANH_2$) and incubated for 20 min at room temperature (RT) to alkylate the sulfhydryl groups. To obtain peptide mixture, proteins were digested by Trypsin Sequencing Grade (Roche, Monza, Italy) in 50 mM AMBIC overnight at 37 °C under stirring (400 rpm). Peptides were purified by reverse phase chromatography, using Zip Tips (µ-C18; Millipore, Milan, Italy).

169 *2.2.2 High resolution mass spectrometry analysis (nLC-MSMS)*

170 Tryptic peptides were analyzed at UNITECH OMICs (University of Milano, Italy) using a Dionex
171 Ultimate 3000 nano-LC system (Sunnyvale CA, USA) connected to an Orbitrap Fusion™ Tribrid™
172 Mass Spectrometer (Thermo Scientific, Bremen, Germany) equipped with a nano-electrospray ion
173 source. Peptide mixtures were pre-concentrated onto an Acclaim PepMap 100 - 100µm x 2cm C18
174 and separated on EASY-Spray column, 15 cm x 75 µm ID packed with Thermo Scientific Acclaim
175 PepMap RSLC C18, 3 µm, 100 Å. The temperature was set to 35 °C and the flow rate was 300 nL
176 min^{-1}. Mobile phases were the following: 0.1% Formic acid (FA) in water (solvent A); 0.1% FA in
177 water/acetonitrile (solvent B) with 2/8 ratio. Peptides were eluted from the column with the
178 following gradient: 4% to 28% of B for 90 min and then 28% to 40% of B in 10 min, and to 95%
179 within the following 6 min to rinse the column. Column was re-equilibrated for 20 min. Total run
180 time was 130 min. One blank was run between triplicates to prevent sample carryover. MS spectra
181 were collected over an m/z range of 375-1500 Da at 120,000 resolutions, operating in the data
182 dependent mode, cycle time 3 sec between master scans. HCD was performed with collision energy
183 set at 35 eV. Each sample was analyzed in three technical triplicates.
184 LTQ raw data was searched against a protein database using SEQUEST algorithm in Proteome
185 Discoverer software version 2.2 (Thermo Scientific) for peptide/protein identification. The searches
186 were performed against Uniprot KnowledgeBase (KB) (taxonomy Bivalvia, 83922 entries). The
187 minimum peptide length was set to six amino acids and enzymatic digestion with trypsin was
188 selected, with maximum 2 missed cleavages. A precursor mass tolerance of 8 ppm and fragment
189 mass tolerance of 0.02 Da were used; acetylation (N-term), oxidation (M) were used as dynamic
190 modifications and carbamidomethylation (C) as static modification. The false discovery rates
191 (FDRs) at the protein and peptide level were set to 0.01 for highly confident peptide-spectrum
192 matches and 0.05 for peptide-spectrum matches with moderate confidence.
193 We considered only proteins with a score of coverage > 2% with at least two identified peptides.
194 Differences in abundance ratio (AR) of proteins between M1 and M2 against control were
195 considered only with at least a 2-fold change and with a standard deviation between replicates less
196 than 20%. We identified 425 different proteins, but the cut-offs made and the necessity of the
197 homology search, based on the "Bivalvia" taxonomy entry only, decreased the proteins to 152.
198

199 RESULTS AND DISCUSSION

200 Although we had previous evidences of the intake of this kind of MPs both in other soft tissues and
201 hemolymph of *D. polymorpha*, as reported in our recent work (Magni et al., 2018), we wanted the
202 certainty of the MPs' presence in the gills to be sure that the potential effects observed on the

proteome were effectively due to these contaminants. Thus, we used the optical microscopy (20x) directly on one of the fresh gills extracted from the mussels collected for the analyses. The microscopy observations pointed out the presence of many MPs of 10 µm interposed among the gill lamellae (Fig. 1 B, C, D) for the two Ms, confirming the uptake capability of zebra mussels also for this physical contaminant. The intake of 1 µm MPs, not visible by optical microscopy, was already observed in this biological model by confocal observations in our previous study (Magni et al., 2018).

Moving to the proteomics' results, no proteins' modulation was obtained at the end of the exposure to M1 in comparison to controls, while M2 was able to modulate 78 different proteins (Fig. 2), but one of the most relevant results concerned the fact that 18 proteins were completely not expressed in zebra mussels exposed to M2 compared to controls (Tab. 1).

The two Ms showed a very different impact on zebra mussels' gill proteome considering the lack of changes observed for the exposure to M1 compared to the heavy effect made by M2, which contain an MPs' concentration only four times greater. This seems to suggest a kind of threshold whose reasons can be simply related to the higher intake of MPs in the mussels that reached the level-threshold to be toxic, but maybe also to the overrun of homeostatic responses that are no longer able to fight the injuries made by MPs. This result, which is the first evidence of this kind of effect due to MPs on the proteome of freshwater organisms, surely opens new questions on the toxicological behavior due to these physical contaminants and maybe can represent the first step to identify hypothetic limits to the environmental concentrations of MPs to be used in a future risk management. Other additional experiments will certainly be needed to confirm the threshold we found, bearing in mind the inability to measure the MPs' concentrations directly in the exposure beakers, as well explained in the paragraph 2.1.

Moving to the modulation of gill protein, we did not observe a specific metabolic pathway as target, but rather a diffuse effect on many protein classes. Figure 3 shows that the catalytic activity (27%) and nucleotide binding were the major classes of proteins modified by the M2 exposure, followed by proteins involved in the structural molecule activity (12%) and protein binding (11%). Proteins related to RNA (5%) and metal ion (4%) bindings close the list of modulated protein classes. More in detail, the changed proteins are mainly involved in the structure and function of ribosomes, energy metabolism, cellular trafficking, RNA-binding and cytoskeleton (Tab. 1), which are directly or indirectly involved in the oxidative stress homeostasis. Indeed, several recent studies highlighted that the increase of oxidative stress and the consequent imbalance of the antioxidant defense mechanism are one of the major effects made by MPs (Jeong et al., 2017; Magara et al., 2018; Yu et al., 2018) probably due to both their intrinsic toxicological effects and the mechanic injuries made

by these physical pollutants that increase the inflammatory status (Jin et al., 2018). The only comparison with other proteomic data is possible with results recently made by Green and co-workers (2019) which however evaluate the effects of other MPs (polylactic acid and polyethylene) in the marine *Mytilus edulis*. Furthermore, comparisons among MPs' impact are more difficult than those made by chemicals since uptake and toxicological effects can be influenced by other physical variables, mainly size and shape. Anyway, the authors found some of the same protein classes modulated by M2, such as proteins involved in the cellular structure, DNA binding, detoxification (e.g. metal ion binding) and metabolism, but also another specific class not modulated by M2 linked to immune response (Green et al., 2018).

In detail, we found an up-regulation of the glutathione reductase (7.8-fold increase; Tab. 1) which suggests the activation of the antioxidant defense chain in the mussel gills. Glutathione reductase (*Gsr*) is a highly-conserved protein involved in the regulation, modulation and maintenance of cellular redox homeostasis by the transformation of oxidized glutathione into its reduced form (Couto et al., 2016). The up-regulation of *Gsr* suggests the attempt of zebra mussels to increase the production of reduced glutathione that is a direct scavenger of OH° and other cell radicals and one of the substrates involved in the glutathione machinery to counteract the oxidative stress.

Another indication of this mechanism of action can be seen through the modulation of the cytoskeleton proteins (Tab. 1) which were always found as one of the major targets of some xenobiotics in different model organisms (Miura et al., 2005; Hanisch et al., 2010; Riva et al., 2012; Binelli et al., 2013). This kind of proteins, which are involved in the maintenance of cell shape, locomotion, intracellular organization and transport, have been indicated as one of the first targets of the oxidative stress (Riva et al., 2012; Wilson et al., 2015; Belcastro et al., 2017). The M2 modulated 11 different proteins directly ascribable to cytoskeleton functions (Tab. 1). In detail, 5 of them were up-regulated: actin-related protein 2/3 complex subunit 2, K1PPK1; myosin-Ie, K1QZI3; tubulin β chain, A0A194AQ74; 33 kDa inner dynein arm light chain, K1PNS2; dynein light chain roadblock, A0A210QUP6; 2 proteins were down-regulated (tropomyosin 1, H6BD84; α-actinin, K1RH58) and 4 of them were not expressed (actin, A0A161HPY5; β-actin, A0A142IJP6; tubulin α chain, K1QII6; septin-2, K1PY30), in the exposed bivalves (Fig. 2 and Tab. 1). It is well known that oxidative stress induces the breakage of F-actin, impairing the microtubule polymerization (Wilson et al., 2015) and that tubulins α and β chain contain many cysteine residues that can be oxidized by endogenous and exogenous oxidizing agents (Landino et al., 2004). The tubulins α chain (*Tuba*) and β chain (*Tubb*) were modulated by the exposure to M2 in different way: the former was completely not expressed (Tab. 1), while the latter was the protein most up-regulated (Tab. 1; Fig. 2). The block of expression for *Tuba* is a dramatic event because it normally binds the

other dimer β to form the microtubules. M2 seems not only to interfere on the microtubules' assemblage, modifying the cellular stability and organization, but could alter also the mechanical defense of the digestive tract of zebra mussel. Indeed, *Tuba* and *Tubb* are also the main components of cilia, which in mussels are present mainly in the syphons with the task to reject dangerous particles, such as diatom frustules and large particulate matter, and facilitate respiration (Magi et al., 2008).

Another effect noticed after the exposure to M2 was the impact on many proteins directly and indirectly involved in the RNA translation and protein synthesis. We found 7 RNA-binding proteins modulated (Tab. 1), 4 of them up-regulated (putative eukaryotic initiation factor 4A-II, A0A194AJS2; eukaryotic initiation factor 4A-III, K1BPL2; GTP-binding nuclear protein, A0A1L5JFM5; small nuclear ribonucleoprotein Sm D3, K1QVD0), 2 proteins down-regulated (polyadenylate-binding protein, K1RJH5; small nuclear ribonucleoprotein Sm D2, A0A210R719) and the RNA-binding protein Nova-1 (A0A210R485) not expressed (Fig.2 and Tab.1).

The RNA-binding proteins (RBPs) play a crucial role in the regulation of gene expression, mainly based on splicing regulation, mRNA transport, modulation of mRNA translation and also in decay. Furthermore, RBPs are strictly involved in response to stress (Alves and Goldenberg, 2016) since it is crucial for the cell to control and arrest mRNA translation during stressful situations, as shown by Holcik and Sonenberg (2005) who indicated as 50% of cell energy is consumed during translation. In particular, the RBPs are one of the main constituents of the so-called stress granules (SGs), which are formed in cytoplasm of cells exposed to many environmental stressors, such as hypoxia, UV, heat and oxidative stress (Anderson and Kedersha, 2006). The role played by SGs was confirmed by the observation of their rapid induction, estimated in 15-30 minutes, in the cell cytoplasm of different model-organisms exposed to different stressors (Mangiardi et al., 2004; Moeller et al., 2004; Kayali et al., 2005). During stress, most mRNAs are directed to either the degradation machinery or SGs, where they remain untranslated until homeostatic conditions are reactivated (Alves and Goldenberg, 2016). SGs are composed by an assemblage of different proteins, that include also the eukaryotic initiation factors (*EiFs*), some ribosomal subunits, scaffold proteins, RNA-stability proteins and many others (Wheeler et al., 2017). It is interesting to note that some proteins included in the classes forming SGs were effectively modulated by M2. Specifically, 2 *EiFs* were up-regulated (*EiF 4A-II* A0A194AJS2 and *EiF 4A-III, K1PBL2*) and one of them was not expressed (putative *EiF 1-like*, A0A194AJY7), as shown in table 1.

Very interestingly, almost all the ribosomal proteins were up-regulated (Tab. 1), confirming the over-production of these proteins' class necessary for the SG formation and considered markers of these cytoplasmic structures (Kedersha and Anderson; 2002). Another evidence of this possible

defense mechanism can be highlighted in the lack of expression of many proteins. Table 1 shows that three heat shock proteins (*Hsps*) were below the detection limit (Heat shock cognate 70 kDa protein, B4E3Z6; Heat shock protein 70, M4GLN4; Putative heat shock protein 90) compared to controls and one was down-regulated (HSP90 protein, A0A023W7V2), while only one was up-regulated (Heat shock cognate 70, A0A0M4TZ63). The *Hsps* are involved in many cell activities, such as folding/unfolding of proteins, cell-cycle control and signaling, protein transport and protection against stress and apoptosis (Li and Srivanstava, 2004). Although several studies highlighted an activation of the *Hsps* related to the increasing oxidative stress (Oksala et al., 2014; Liu et al., 2015; Wang et al., 2018; Ikwegbue et al., 2018), our proteomics results seem to show a more complicated situation. Indeed, if the "silver thread" among the modulation of the different protein classes made by M2 is effectively the activation of the response machinery against the oxidative stress, the inactivation or down-regulation of *Hsps* seems to be inconsistent. Actually, the modulation of *Hsps* noticed could be simply related to one of the numerous other functions above described, but the most intriguing explanation concerns the physical nature of the administered contaminant that can trigger a different cascade of events than that produced by chemical pollutants. Since a background level of these *Hsps* was evaluated in the controls, the complete blockage of their expression could point out that cells consider them as housekeeping proteins, whose mRNA must be untranslated for cellular energy-saving, instead of possible barrier against the injuries made by M2 exposure. Another evidence on the response based on the energy pathways was the modulation of some proteins related to energy source and production, whose 4 of them were down-regulated, 4 up-regulated and one not expressed (Tab. 1). More specifically, 5 proteins (isocitrate dehydrogenase, K1R7T2; enolase, K1QX37; phosphoglycerate kinase, K1QCC1; fructose-bisphosphate aldolase, K1R8R6 and GAPDH, A0A2H4NFY0) were directly involved in the glycolysis and one in the Krebs cycle (methylmalonyl-CoA mutase, K1QE55), showing as M2 was able to interfere also on the cellular energetic balance. Indeed, similar results were obtained in a previous study (Sussarellu et al., 2016) in which polystyrene microparticles were administered to Pacific oysters, interfering with energy uptake and allocation. This negative effect shifted the energy flows toward organism maintenance and structural growth at the expense of reproduction.

Lastly, the last big protein class modulated by M2 was related to protein degradation with 3 proteins up-regulated, 3 down-regulated and one not expressed (Tab. 1). In detail, 3 of them (26S proteasome non-ATPase regulatory subunit 7, A0A210QH02; 26S proteasome non-ATPase regulatory subunit 14, A0A210QNI0; proteasome subunit α type, K1R6F1) are components of the proteasome, a multiprotein complex mainly involved in the ATP-dependent degradation of ubiquitinated proteins.

In summary, even if some evidences must be confirmed, for instance through microscopy observations for the probable formation of SGs, our results confirmed the sensitivity of the proteomic approach in ecotoxicology and its capability to highlight the adverse effects made also by these physical contaminants. In particular, this methodology suggested that M2 was able to create an imbalance in the oxidative status of gill cells which was reflected in the modulation of many proteins involved in some different cellular pathways, as summarized in figure 4.

CONCLUSIONS

This study adds another brick in the knowledge of the risk assessment associated to virgin MPs. One of the pivotal results is the discovery of a "quantal effect" demonstrated by a clear threshold between M1 and M2, situation absolutely not predictable before the exposures and never described in the previous studies on MPs. Proteomics performed this task very well, proving its sensitivity and the capability to investigate the deepest effects due to M2 that modulate especially proteins belonging to 5 different classes involved in crucial cellular pathways. The ultimate effect which connects the modulation of these protein classes seemed to be the increase of oxidative stress and the related activation of the antioxidant machinery.

Our data drive to other in-depth studies, based on different techniques, to evaluate if the biochemical effects noticed could determine negative consequences also at the higher levels of the biological scale. Moreover, other experiments should be conducted considering also the possible adsorption of phytoplankton and/or environmental pollutants to MPs that can modify both their aggregation and bioavailability.

REFERENCES

Allsopp, M., Walters, A., Santillo, D., Johnsto, P., 2006. Plastic Debris in the World's Oceans. Greenpeace International, Amsterdam, Netherlands.

Alves, L.R., Goldenberg, S., 2016. RNA-binding proteins related to stress response and differentiation in protozoa. World Journal of Biological Chemistry 26, 78-87.

Anderson, P., Kedersha, N., 2006. RNA granules. Journal of Cell Biology 172, 803-808.

Bakir, A., Rowland, S.J., Thompson, R.C, 2014. Enhanced desorption of persistent organic pollutants from microplastics under simulated physiological conditions. Environmental Pollution 185, 16-23.

Belcastro, E., Wu, W., Fries-Raeth, I., Corti, A., Pompella, A., Leroy, P., Larteaud, I., Gaucher, C., 2017. Oxidative stress enhances and modulates protein S-nitrosation in smooth muscle cells exposed to S-nitrosoglutathione. Nitric Oxide 69, 10-21.

373 Binelli, A., Del Giacco, L., Santo, N., Bini, L., Magni, S., Parolini, M., Madaschi, L., Ghilardi, A.,
374 Maggioni, D., Ascagni, M., Armini, A., Prosperi, L., Landi, L., La Porta, C., Della Torre, C.,
375 2017. Carbon nanopowder acts as a Trojan-horse for benzo(α)pyrene in *Danio rerio* embryos.
376 Nanotoxicology 11, 371-381.
377 Binelli, A., Della Torre, C., Magni, S., Parolini, M., 2015. Does zebra mussel (*Dreissena*
378 *polymorpha*) represent the freshwater counterpart of *Mytilus* in ecotoxicological studies? A
379 critical review. Environmental Pollution 196, 386-403.
380 Binelli, A., Marisa, I., Fedorova, M., Hoffmann, R., Riva, C., 2013. First evidence of protein profile
381 alteration due to the main cocaine metabolite (benzoylecgonine) in a freshwater biological
382 model. Aquatic Toxicology 140-141, 268-278.
383 Bradford, M.M., 1976. A rapid and sensitive method for the quantification of microgram quantities
384 of protein using the principle of protein-dye binding. Analytical Biochemistry 72, 248-254.
385 Browne, M.A., Galloway, T., Thompson, RC., 2007. Microplastic-an emerging contaminant of
386 potential concern? Integrated Environmental Assessment and Management 3, 559-566.
387 Carr, S.A., Liu, J., Tesoro, A.G., 2016. Transport and fate of microplastic particles in wastewater
388 treatment plants. Water Research 91, 174-182.
389 Chen, Q., Gundlach, M., Yang, S., Jiang, J., Velki, M., Yin, D., Hollert, H., 2017. Quantitative
390 investigation of the mechanisms of microplastics and nanoplastics toward zebrafish larvae
391 locomotor activity. Science of the Total Environment. 584-585, 1022-1031.
392 Cole, M., Lindeque, P., Halsband, C., Galloway, T.S., 2011. Microplastics as contaminants in the
393 marine environment: a review. Marine Pollution Bulletin 62, 2588-2597.
394 Couto, N., Wood, J., Barber, J., 2016. The role of glutathione reductase and related enzymes on
395 cellular redox homoeostasis network. Free Radical Biology Medicine 95, 27-42.
396 Ding, J., Zhang, S., Razanajatovo, R.M., Zou, H., 2018. Accumulation, tissue distribution, and
397 biochemical effects of polystyrene microplastics in the freshwater fish red tilapia (*Oreochromis*
398 *niloticus*). Environmental Pollution 238, 1-9.
399 Eerkes-Medrano, D., Thompson, R.C., Aldridge, D.C., 2015. Microplastics in freshwater systems: a
400 review of the emerging threats, identification of knowledge gaps and prioritization of research
401 needs. Water Research 75, 63-82.
402 Green, D.S., Colgan, T.J., Thompson, R.C., Carolan, J.C., 2019. Exposure to microplastics reduces
403 attachment strength and alters the haemolymph proteome of blue mussels (*Mytilus edulis*).
404 Environmental Pollution 246, 423-434.
405 Guilhermino, L., Vieira, L.R., Ribeiro, D., Tavares, A.S., Cardoso, V., Alves, A., Almeida, J.M.,
406 2018. Uptake and effects of the antimicrobial florfenicol, micro- plastics and their mixtures on

freshwater exotic invasive bivalve *Corbicula fluminea*. Science of the Total Environment 622-623, 1131-1142.

Hammer, J., Kraak, M.H.S., Parsons, J.R., 2012. Plastics in the marine environment: the dark side of a modern gift, in: Whitacre D.M. (Ed.), reviews of environmental contamination and toxicology. Springer, New York, pp. 1-44.

Hanisch, K., Küster, E., Altenburger, R., Gündel, U., 2010. Proteomic signatures of the Zebrafish (*Danio rerio*) embryo: sensitivity and specificity in toxicity assessment of chemicals. International Journal of Proteomics 630134.

Hartmann, N.B., Huffer, T., Thompson, R.C., Hasselov, M., Verschoor, A., Daugaard, A.E., Rist, S., Karlsson, T., Brennholt, N., Cole, M., Herrling, M.P., Hess, M.C., Ivleva, N.P., Lusher, A.L., Wagner, M., 2019. Are We Speaking the Same Language? Recommendations for a Definition and Categorization Framework for Plastic Debris. Environmental Science & Technology 53, 1039-1047.

Hidalgo-Ruz, V., Gutow, L., Thompson, R.C., Thiel, M., 2012. Microplastics in the marine environment: a review of the methods used for identification and quantification. Environmental Science & Technology 46, 3060-3075.

Holcik, M., Sonenberg, N., 2005. Translational control in stress and apoptosis. Nature Reviews Molecular Cell Biology 6, 318-327.

Ikwegbue, P.C., Masamba, P., Oyinloye, B.E., Kappo, A.P., 2018. Roles of heat shock proteins in apoptosis, oxidative Stress, human inflammatory diseases, and cancer. Pharmaceuticals 11, 2.

Jeong, C.B., Kang, H.M., Lee, M.C., Kim, D.H., Han, J., Hwang, D.S., Souissi, S., Lee, S.J., Shin, K.H., Park, H.G., Lee, JS., 2017. Adverse effects of microplastics and oxidative stress-induced MAPK/Nrf2 pathway-mediated defense mechanisms in the marine copepod *Paracyclopina nana*. Scientific Reports 41323.

Jin, Y.X., Xia, J.Z., Pan, Zh., Jang, J.J., Wang, W.C., 2018. Polystyrene microplastics induce microbiota dysbiosis and inflammation in the gut of adult zebrafish. Environmental Pollution 235, 322-329.

Jovanovic, B., 2017. Ingestion of microplastics by fish and its potential consequences from a physical perspective. Integrated Environmental Assessment and Management 13 (3), 510-515.

Kayali, F., Montie, H.L., Rafols, J.A., De Gracia, D.J., 2005. Prolonged translation arrest in reperfused hippocampal cornu Ammonis 1 is mediated by stress granules. Neuroscience 134, 1223-1245.

Kedersha, N., Anderson, P., 2002. Stress granules: sites of mRNA triage that regulate mRNA stability and translatability. Biochemical Society Transactions 30, 963-969.

441 Lambert, S., Wagner, M., 2018. Freshwater Microplastics. Springer International Publishing, Cham,
442 Switzerland.
443 Landino, L.M., Moynihan, K.L., Todd, J.V., Kennett, K.L., 2004. Modulation of the redox state of
444 tubulin by the glutathione/glutaredoxin reductase system. Biochemical and Biophysical Research
445 Communications 314, 555-560.
446 Lei, L., Wu, S., Lu, S., Liu, M., Song, Y., Fu, Z., Shi, H., Raley-Susman, K.M., He, D., 2018.
447 Microplastic particles cause intestinal damage and other adverse effects in zebrafish *Danio rerio*
448 and nematode *Caenorhabditis elegans*. Science of the Total Environment 619-620, 1-8.
449 Li, J., Liu, H., Chen, J.P., 2018. Microplastics in freshwater systems: a review on occurrence,
450 environmental effects, and methods for microplastics detection. Water Research 137, 362-374.
451 Li, Z., Srivastava, P., 2004. Heat-shock proteins. Current Protocols in Immunology 58, A.1T.1-
452 A.1T.6.
453 Liu, C.P., Fu, J., Xu, F.P., Wang, X.S., Li, S., 2015. The role of heat shock proteins in oxidative
454 stress damage induced by Se deficiency in chicken livers. Biometals 28, 163-173.
455 Lu, Y., Zhang, Y., Deng, Y., Jiang, W., Zhao, Y., Geng, J., Ding, L., Ren, H., 2016. Uptake and
456 accumulation of polystyrene microplastics in zebrafish (*Danio rerio*) and toxic effects in liver.
457 Environmental Science & Technology 50, 4054-4060.
458 Magara, G., Elia, A.C., Syberg, K., Khan, FR., 2018. Single contaminant and combined exposures
459 of polyethylene microplastics and fluoranthene: accumulation and oxidative stress response in
460 the blue mussel, *Mytilus edulis*. Journal of Toxicology and Environmental Health Part A 81,
461 761-733.
462 Magi, E., Liscio, C., Pistarino, E., Santamaria, B., Di Carro, M., Tiso, M., Scaloni, M., Renzone,
463 G., Cosulich, M.E., 2008. Interdisciplinary study for the evaluation of biochemical alterations on
464 mussel *Mytilus galloprovincialis* exposed to a tributyltin-polluted area. Analytical and
465 Bioanalytical Chemistry 391, 671-678.
466 Magni, S., Gagné, F., André, C., Della Torre, C., Auclair, J., Hanana, H., Parenti, C.C., Bonasoro,
467 F., Binelli, A., 2018. Evaluation of uptake and chronic toxicity of virgin polystyrene microbeads
468 in freshwater zebra mussel *Dreissena polymorpha* (Mollusca: Bivalvia). Science of the Total
469 Environment 631-632, 778-788.
470 Magni, S., Parolini, M., Binelli, A., 2016. Sublethal effects induced by morphine to the freshwater
471 biological model *Dreissena polymorpha*, Environmental Toxicology 31, 58-67.
472 Magni, S., Parolini, M., Della Torre, C., de Oliveira, L. F., Catani, M., Guzzinati, R., Cavazzini, A.,
473 Binelli, A., 2017. Multi-biomarker investigation to assess toxicity induced by two
474 antidepressants on *Dreissena polymorpha*. Science of the Total Environment 578, 452-459.

475 Mangiardi, D.A., McLaughlin-Williamson, K., May, K.E., Messana, E.P., Mountain, D.C.,
476 Cotanche, D.A., 2004. Progression of hair cell ejection and molecular markers of apoptosis in
477 the avian cochlea following gentamicin treatment. Journal of Comparative Neurology 475, 1-18.
478 Miura, Y., Kano, M., Abe, K., Urano, S., Suzuki, S., Toda, T., 2005. Age-dependent variations of
479 cell response to oxidative stress: proteomic approach to protein expression and phosphorylation.
480 Electrophoresis 26, 2786-2796.
481 Moeller, B.J., Cao, Y., Li, C.Y., Dewhirst, M.W., 2004. Radiation activates HIF-1 to regulate
482 vascular radiosensitivity in tumors: role of reoxygenation, free radicals, and stress granules.
483 Cancer Cell 5, 429-441.
484 Monsinjor, T., and Knigge, T., 2007. Proteomic applications in ecotoxicology. Proteomics 7, 2997-
485 3009.
486 Oksala, N.K.J., Ekmekci, F.G., Ozsoy, E., Kirankaya, S., Kokkola, T., Emecen, G., Lappalainen, J.,
487 Kaarniranta, K., Atalay, M., 2014. Natural thermal adaptation increases heat shock protein levels
488 and decreases oxidative stress. Redox Biology 3, 25-28.
489 Riva, C., Cristoni, S., Binelli, A., 2012. Effects of Triclosan in the freshwater *Dreissena*
490 *polymorpha*: a proteomic investigation. Aquatic Toxicology 118-119, 62-71.
491 Sleight, V.A., Bakir, A., Thompson, R.C., Henry, T.B., 2017. Assessment of microplastic-sorbed
492 contaminant bioavailability through analysis of biomarker gene expression in larval zebrafish.
493 Marine Pollution Bulletin 116, 291-297.
494 Sussarellu, R., Suquet, M., Thomas, Y., Lambert, C., Fabioux, C., Pernet, M.E.J., Le Goïc, N.,
495 Quillien, V., Mingant, C., Epelboin, Y., Corporeau, C., Guyomarch, J., Robbens, J., Paul-Pont,
496 I., Soudant, P., Huvet, A., 2016. Oyster reproduction is affected by exposure to polystyrene
497 microplastics.
498 Thompson, R.C., Moore, C.J., vom Saal, F.S., Swan, S.H., 2009. Plastics, the environment and
499 human health: current consensus and future trends. Philosophical Transactions of the Royal
500 Society B 364, 2153-2166.
501 Wang, Y., Zhao, H., Liu, J., Shao, Y., Li, J., Luo, L., Xing, M., 2018. Copper and arsenic-induced
502 oxidative stress and immune imbalance are associated with activation of heat shock proteins in
503 chicken intestines. International Immunopharmacology 60, 64-75.
504 Weber, A., Scherer, C., Brennholt, N., Reifferscheid, G., Wagner, M., 2018. PET microplastics do
505 not negatively affect the survival, development, metabolism and feeding activity of the
506 freshwater invertebrate *Gammarus pulex*. Environmental Pollution 234, 181-189.
507 Wheeler, J.R., Jain, S., Khong, A., Parker, R., 2017. Isolation of yeast and mammalian stress
508 granule cores. Methods 126, 12-17.

509 Wilson, C., Gonzalez-Billault, C., 2015. Regulation of cytoskeletal dynamics by redox signaling
510 and oxidative stress: implications for neuronal development and trafficking. Frontiers in Cellular
511 Neuroscience 9, 381.
512 Yu, P., Liu, ZQ., Wu, D.L., Chen, M.H., Lv, W.W., Zhao, Y.L., 2018. Accumulation of polystyrene
513 microplastics in juvenile *Eriocheir sinensis* and oxidative stress effects in the liver. Aquatic
514 Toxicology 200, 28-36.

CAPTIONS

Figure 1 **Intake of MPs:** microplastics of 10 μm (indicated by arrows) inserted in the gills' lamellae of zebra mussels (B, C, D) in comparison to controls (A). fs=frontal surface of a filament; is=interfilament space.

Figure 2 **Protein profiling modulation:** differentially modulated proteins due to M1 and M2 related to controls.

Figure 3 **Molecular function of modulated proteins:** gene ontology analyses of identified proteins in M1 and M2. The showed enriched categories are related to the molecular functions of gills' proteins.

Figure 4 **Proteins' classes affected by M2:** Summarizing scheme of the suggested mechanism of action with the main proteins' classes modulated by the M2 exposure. *Gsr* = glutathione reductase; *Tuba* = tubulin α chain; *Tubb* = tubulin β chain; *EiFs* = eukaryotic initiation factors.

Table 1 Description of the proteins modulated in the zebra mussel gills by M1 and M2.

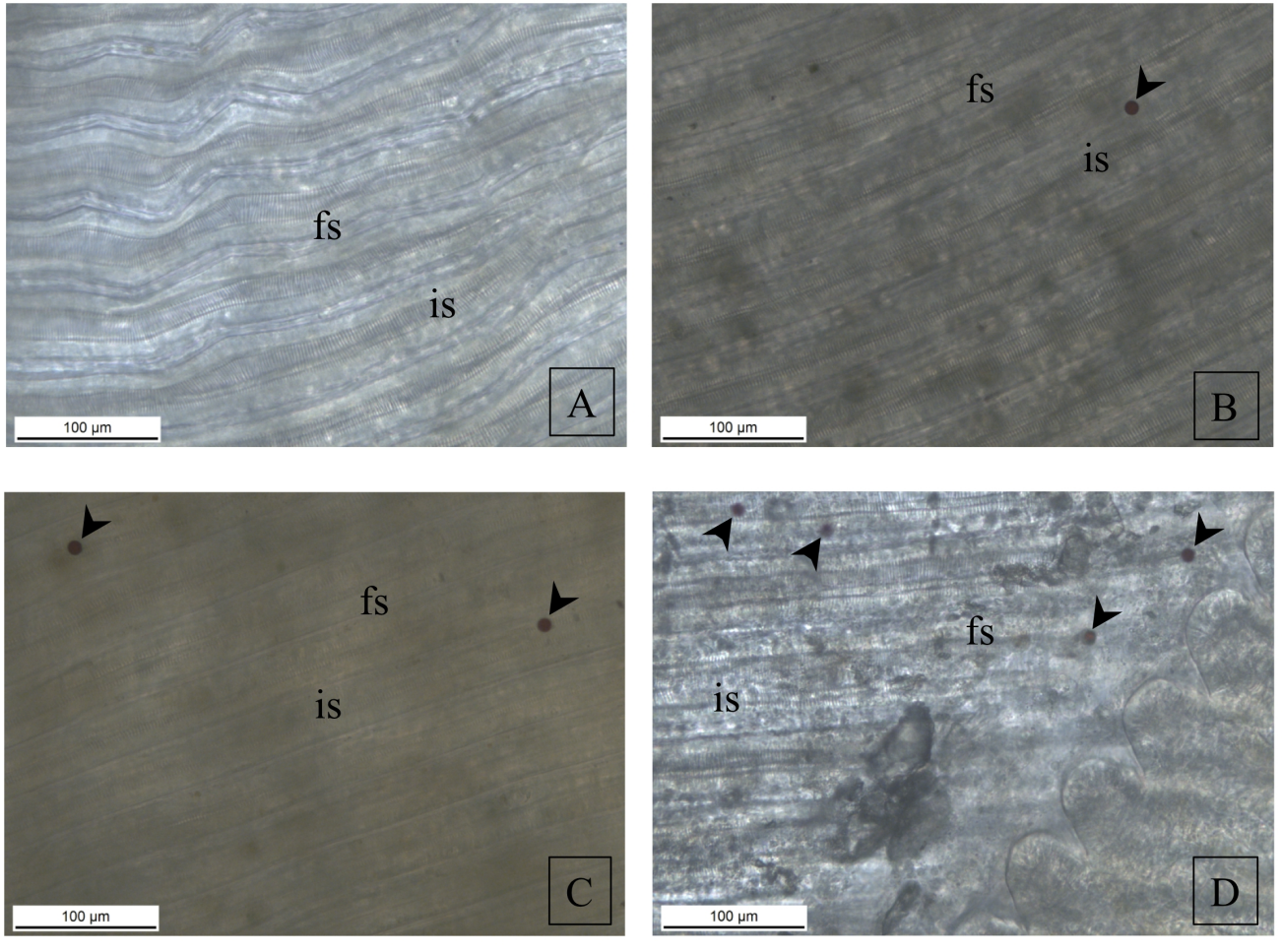
fs
is
100 µm
A
fs
is
100 µm
B
fs
is
100 µm
C
fs
is
100 µm
D

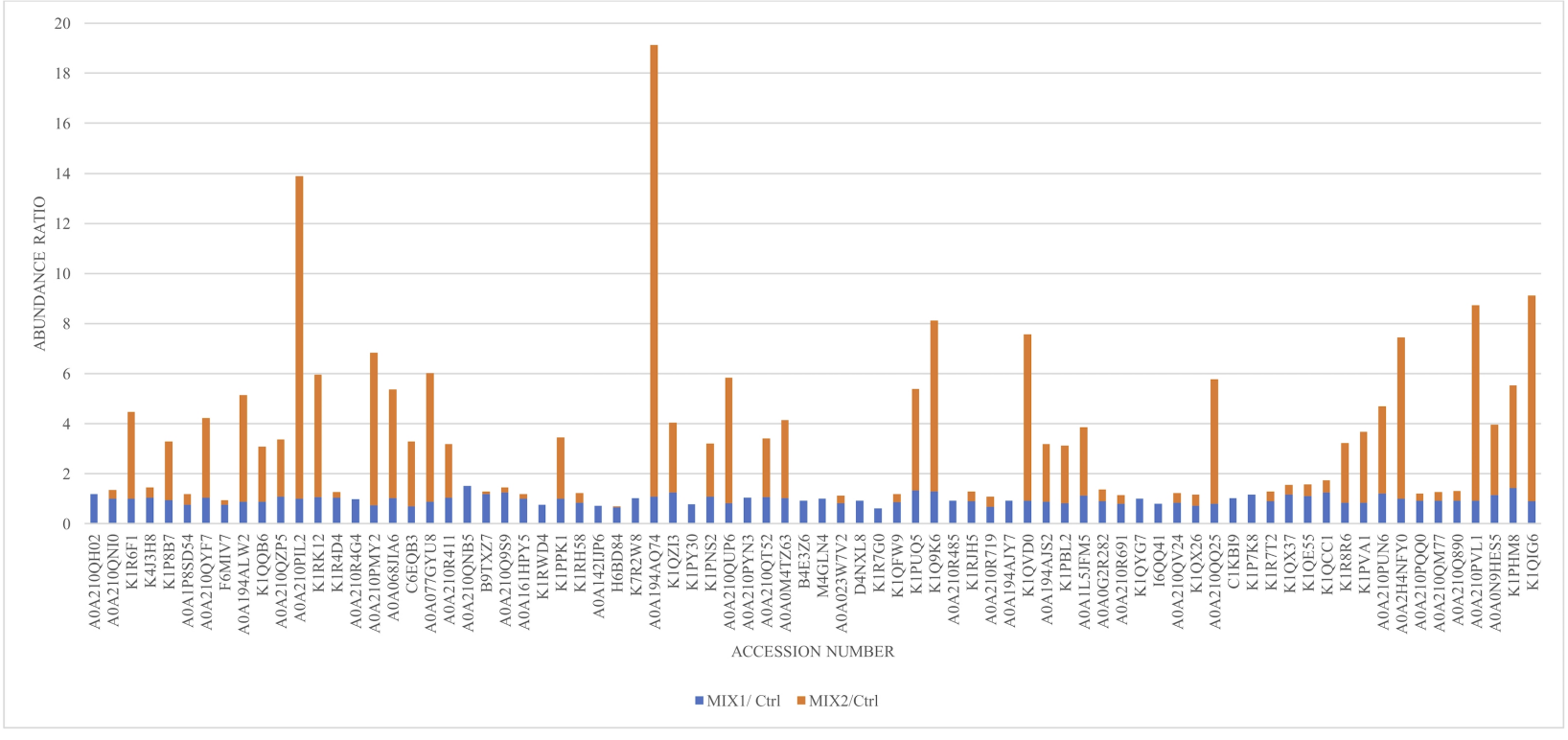
ABUNDANCE RATIO
20
18
16
14
12
10
8
6
4
2
0
A0A210QH02
A0A210QNI0
K1R6F1
K4J3H8
K1P8B7
A0A1P8SD54
A0A210QYF7
F6MIV7
A0A194ALW2
K1QQB6
A0A210QZP5
A0A210PIL2
K1RK12
K1R4D4
A0A210R4G4
A0A210PMY2
A0A068JIA6
C6EQB3
A0A077GYU8
A0A210R411
A0A210QNB5
B9TXZ7
A0A210Q9S9
A0A161HPY5
K1RWD4
K1PPK1
K1RH58
A0A1421JP6
H6BD84
K7R2W8
A0A194AQ74
K1QZI3
K1PY30
K1PNS2
A0A210QUP6
A0A210PYN3
A0A210QT52
A0A0M4TZ63
B4E3Z6
M4GLN4
A0A023W7V2
D4NXL8
K1R7G0
K1QFW9
K1PUQ5
K1Q9K6
A0A210R485
K1RJH5
A0A210R719
A0A194AJY7
K1QVD0
A0A194AJS2
K1PBL2
A0A1L5JFM5
A0A0G2R282
A0A210R691
K1QYG7
I6QQ41
A0A210QV24
K1QX26
A0A210QQ25
C1KBI9
K1P7K8
K1R7T2
K1QX37
K1QE55
K1QCC1
K1R8R6
K1PVA1
A0A210PUN6
A0A2H4NFY0
A0A210PQQ0
A0A210QM77
A0A210Q890
A0A210PVL1
A0A0N9HES5
K1PHM8
K1QIG6
ACCESSION NUMBER
MIX1/ Ctrl
MIX2/Ctrl

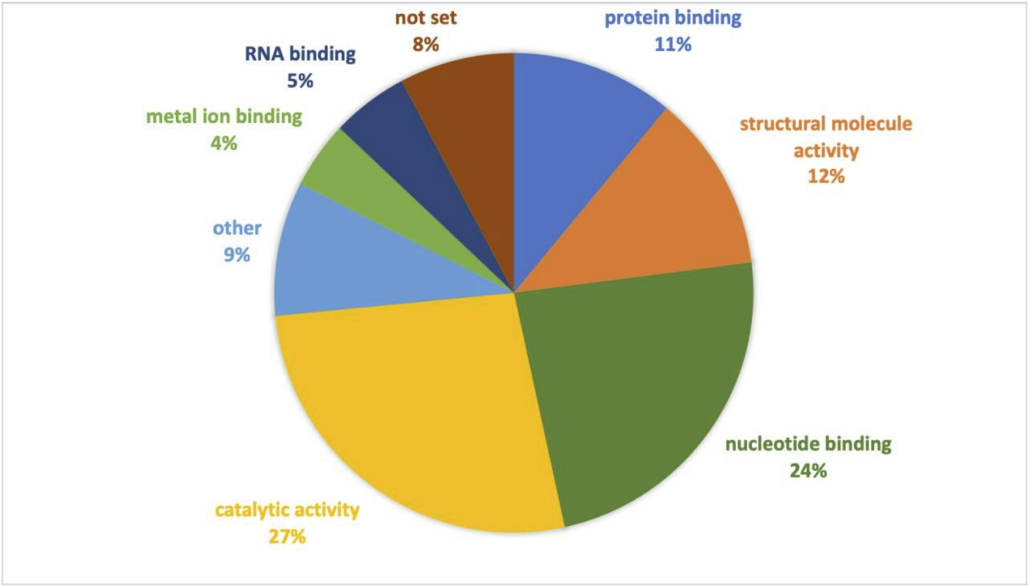
not set
8%
protein binding
11%
RNA binding
5%
metal ion binding
4%
structural molecule
activity
12%
other
9%
nucleotide binding
24%
catalytic activity
27%

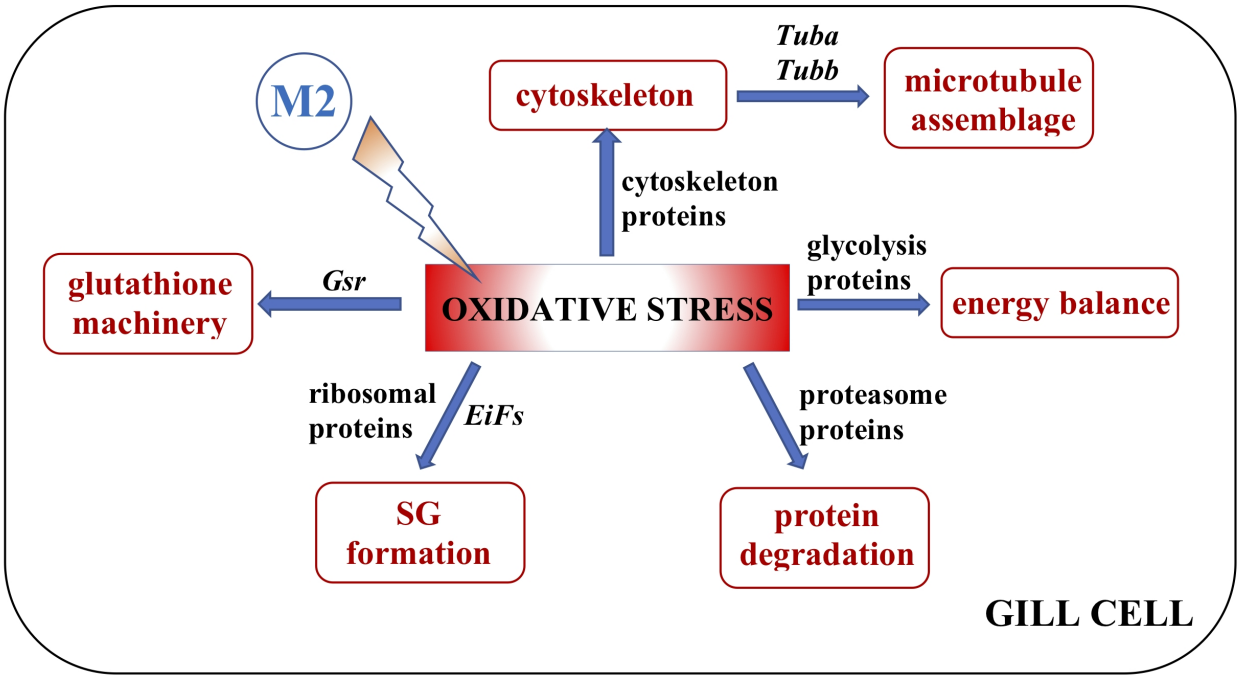
M2
cytoskeleton
Tuba
Tubb
microtubule assemblage
cytoskeleton proteins
glutathione machinery
Gsr
OXIDATIVE STRESS
glycolysis proteins
energy balance
ribosomal proteins
EiFs
proteasome proteins
SG formation
protein degradation
GILL CELL

Main Function	UniProt Accession	Description	Coverage [%]	Peptides	Unique Peptides	MW [kDa]	pI	AR: (M1) / (Ctrl)	AR: (M2) / (Ctrl)
Protein degradation	A0A210QH02	26S proteasome non-ATPase regulatory subunit 7 (*Mizuhopecten yessoensis*)	9	2	2	38.1	6.62	1.180	NOT FOUND
	A0A210QNI0	26S proteasome non-ATPase regulatory subunit 14 (*Mizuhopecten yessoensis*)	6	2	2	34.6	6.58	0.998	0.349
	K1R6F1	Proteasome subunit alpha type (*Crassostrea gigas*)	31	6	6	28.0	7.47	0.995	3.466
	K4J3H8	Activated protein kinase C receptor (Fragment) (*Solen grandis*)	23	6	5	26.5	8.63	1.040	0.403
	K1P8B7	Ubiquitin-conjugating enzyme E2-17 kDa (Fragment) (*Crassostrea gigas*)	40	3	3	14.7	5.41	0.930	2.344
	A0A1P8SD54	Ubiquitin (*Ruditapes philippinarum*)	86	8	8	8.7	7.25	0.743	0.443
	A0A210QYF7	cAMP-dependent protein kinase regulatory subunit (*Mizuhopecten yessoensis*)	6	2	2	42.2	5.43	1.030	3.187
	F6MIV7	Cathepsin B (*Cristaria plicata*)	4	2	2	38.5	6.10	0.758	0.176
Ribosome structure	A0A194ALW2	40S ribosomal protein S6 (*Pinctada fucata*)	12	4	2	27.9	10.83	0.879	4.252
	K1QQB6	40S ribosomal protein S14 (*Crassostrea gigas*)	25	6	6	16.3	10.36	0.866	2.217
	A0A210QZP5	40S ribosomal protein S17 (*Mizuhopecten yessoensis*)	21	3	3	16.9	9.70	1.071	2.286
	A0A210PIL2	40S ribosomal protein S20 (*Mizuhopecten yessoensis*)	24	2	2	13.7	10.32	1.000	12.887

	K1RK12	40S ribosomal protein S23 (*Crassostrea gigas*)	3	2	2	79.5	7.12	1.054	4.891
	K1R4D4	40S ribosomal protein SA (*Crassostrea gigas*)	38	9	2	33.3	4.92	1.041	0.212
	A0A210R4G4	60S ribosomal protein L18a (*Mizuhopecten yessoensis*)	9	2	2	20.9	10.90	0.979	NOT FOUND
	A0A210PMY2	60S ribosomal protein L36 (*Mizuhopecten yessoensis*)	10	2	2	12.7	11.80	0.725	6.096
	A0A068JIA6	60S ribosomal protein L6 (Fragment) (*Azumapecten farreri*)	9	3	3	24.7	10.54	1.022	4.331
	C6EQB3	Ribosomal protein L8 (Fragment) (*Modiolus modiolus*)	8	2	2	24.4	10.36	0.692	2.586
	A0A077GYU8	Ribosomal protein L19 (Fragment) (*Mytilus trossulus*)	22	6	6	23.8	11.43	0.874	5.134
	A0A194AJY7	Putative eukaryotic translation initiation factor 1-like protein (*Pinctada fucata*)	14	2	2	12.9	8.02	0.924	NOT FOUND
Protein synthesis	A0A210R411	Serine--tRNA ligase, cytoplasmic (*Mizuhopecten yessoensis*)	5	2	2	58.6	6.44	1.046	2.138
	A0A210QNB5	Small nuclear ribonucleoprotein E (*Mizuhopecten yessoensis*)	16	2	2	10.5	9.38	1.515	NOT FOUND
Protein Folding	B9TXZ7	Peptidyl-prolyl cis-trans isomerase (Fragment) (*Dreissena polymorpha*)	63	4	4	8.4	8.51	1.180	0.103
	A0A210Q9S9	Peptidyl-prolyl cis-trans isomerase (*Mizuhopecten yessoensis*)	23	4	4	18.1	8.07	1.251	0.198
Cytoskeleton structure	A0A161HPY5	Actin (*Crassostrea brasiliana*)	94	43	10	41.7	5.48	1.005	0.182

	K1RWD4	Actin, cytoplasmic (*Crassostrea gigas*)	79	40	4	41.9	5.39	0.744	NOT FOUND
	K1PPK1	Actin-related protein 2/3 complex subunit 4 (*Crassostrea gigas*)	13	3	3	19.6	8.92	1.003	2.441
	K1RH58	Alpha-actinin, sarcomeric (*Crassostrea gigas*)	23	19	9	102.1	5.45	0.825	0.402
	A0A142IJP6	Beta-actin (*Sinanodonta woodiana*)	76	36	2	41.8	5.48	0.711	NOT FOUND
	H6BD84	Tropomyosin 1 (Fragment) (*Ostrea edulis*)	13	2	2	16.3	4.88	0.645	0.051
	K7R2W8	Tubulin alpha chain (Fragment) (*Scrobicularia plana*)	43	22	2	50.3	5.20	1.015	NOT FOUND
	A0A194AQ74	Tubulin beta chain (*Pinctada fucata*)	74	32	4	43.3	4.86	1.073	18.064
	K1QZI3	Myosin-Ie (*Crassostrea gigas*)	3	2	2	127.9	9.16	1.233	2.803
	K1PY30	Septin-2 (*Crassostrea gigas*)	4	2	2	72.3	8.81	0.771	NOT FOUND
	K1PNS2	33 kDa inner dynein arm light chain, axonemal (*Crassostrea gigas*)	10	2	2	27.0	9.11	1.074	2.133
	A0A210QUP6	Dynein light chain roadblock (*Mizuhopecten yessoensis*)	18	3	3	11.3	9.41	0.819	5.007
Transport	A0A210PYN3	AP complex subunit beta (*Mizuhopecten yessoensis*)	4	2	2	103.7	5.03	1.043	NOT FOUND
	A0A210QT52	Pleckstrin homology domain-containing family F member 2 (*Mizuhopecten yessoensis*)	9	2	2	26.7	8.00	1.065	2.347
Heat shock proteins	A0A0M4TZ63	Heat shock cognate 70 (*Septifer virgatus*)	28	18	3	71.2	5.43	1.019	3.114

	B4E3Z6	Heat shock cognate 70 kDa protein (Fragment) (*Laternula elliptica*)	33	4	2	12.3	8.38	0.912	NOT FOUND
	M4GLN4	Heat shock protein 70 (*Sinonovacula constricta*)	28	20	3	70.9	5.41	0.995	NOT FOUND
	A0A023W7V2	HSP90 protein (*Ruditapes philippinarum*)	19	13	4	83.6	4.93	0.807	0.302
	D4NXL8	Putative heat shock protein 90 (Fragment) (*Dreissena polymorpha*)	56	6	3	11.5	5.19	0.919	NOT FOUND
Binding proteins	K1R7G0	Chromobox-like protein 5 (*Crassostrea gigas*)	13	2	2	22.4	4.91	0.616	NOT FOUND
	K1QFW9	Uncharacterized protein (*Crassostrea gigas*)	5	3	3	94.8	7.06	0.846	0.337
DNA-binding proteins	K1PUQ5	Histone H2B (*Crassostrea gigas*)	35	5	5	13.7	10.59	1.331	4.047
	K1Q9K6	Histone H3 (*Crassostrea gigas*)	13	3	3	28.9	10.62	1.276	6.833
RNA-binding proteins	A0A210R485	RNA-binding protein Nova-1 (*Mizuhopecten yessoensis*)	4	2	2	66.6	6.80	0.909	NOT FOUND
	K1RJH5	Polyadenylate-binding protein (*Crassostrea gigas*)	9	5	5	71.6	9.41	0.904	0.373
	A0A210R719	Small nuclear ribonucleoprotein Sm D2 (*Mizuhopecten yessoensis*)	33	2	2	13.7	9.95	0.670	0.406
	K1QVD0	Small nuclear ribonucleoprotein Sm D3 (*Crassostrea gigas*)	11	3	3	14.2	10.54	0.923	6.645
	A0A194AJS2	Putative eukaryotic initiation factor 4A-II (*Pinctada fucata*)	24	4	4	28.5	5.83	0.865	2.317
	K1PBL2	Eukaryotic initiation factor 4A-III (*Crassostrea gigas*)	3	3	3	137.7	7.18	0.809	2.319

	A0A1L5JFM5	GTP-binding nuclear protein (*Paphia undulata*)	28	7	7	24.8	6.92	1.121	2.73
Calcium-binding proteins	A0A0G2R282	Calmodulin (Fragment) (*Isognomon nucleus*)	61	4	3	12.4	4.23	0.894	0.475
	A0A210R691	Calmodulin (*Mizuhopecten yessoensis*)	21	2	2	16.8	4.34	0.785	0.362
Biosynthesis	K1QYG7	Glucosamine--fructose-6-phosphate aminotransferase [isomerizing] 1 (*Crassostrea gigas*)	5	2	2	81.9	6.80	0.996	NOT FOUND
Chaperones	I6QQ41	Protein disulfide-isomerase (*Mytilus galloprovincialis*)	7	3	3	55.1	4.65	0.797	NOT FOUND
	A0A210QV24	78 kDa glucose-regulated protein (*Mizuhopecten yessoensis*)	22	9	2	72.7	5.05	0.836	0.392
	K1QX26	Endoplasmin (*Crassostrea gigas*)	3	4	2	125.3	4.97	0.712	0.456
	A0A210QQ25	T-complex protein 1 subunit eta (*Mizuhopecten yessoensis*)	11	4	4	59.4	6.21	0.801	4.968
Trafficking	C1KBI9	Rab7-like protein (*Pinctada martensii*)	12	2	2	23.1	5.48	1.024	NOT FOUND
Energy source/production	K1P7K8	Vesicle-fusing ATPase 1 (*Crassostrea gigas*)	3	2	2	82.7	6.77	1.154	NOT FOUND
	K1R7T2	Isocitrate dehydrogenase [NADP] (*Crassostrea gigas*)	6	2	2	46.3	6.55	0.900	0.374
	K1QX37	Enolase (*Crassostrea gigas*)	5	4	4	127.3	7.34	1.164	0.388
	K1QE55	Methylmalonyl-CoA mutase, mitochondrial (*Crassostrea gigas*)	4	2	2	81.7	5.90	1.106	0.455

	K1QCC1	Phosphoglycerate kinase (*Crassostrea gigas*)	7	2	2	43.0	7.72	1.246	0.490
	K1R8R6	Fructose-bisphosphate aldolase (*Crassostrea gigas*)	11	4	4	43.5	6.20	0.834	2.385
	K1PVA1	Transitional endoplasmic reticulum ATPase (*Crassostrea gigas*)	24	16	5	88.6	5.30	0.832	2.827
	A0A210PUN6	V-type proton ATPase subunit E (*Mizuhopecten yessoensis*)	5	2	2	26.1	7.03	1.199	3.480
	A0A2H4NFY0	GAPDH (Fragment) (*Ruditapes philippinarum*)	12	3	3	20.0	8.35	0.998	6.448
Signaling	A0A210PQQ0	Serine/threonine-protein phosphatase (*Mizuhopecten yessoensis*)	12	3	3	41.1	5.17	0.916	0.282
	A0A210QM77	Glutamate dehydrogenase (*Mizuhopecten yessoensis*)	6	3	3	59.5	7.93	0.907	0.357
	A0A210Q890	Major vault protein (*Mizuhopecten yessoensis*)	11	8	8	96.4	5.94	0.915	0.387
Antioxidant activity	A0A210PVL1	Glutathione reductase (*Mizuhopecten yessoensis*)	3	2	2	49.1	6.87	0.921	7.806
Multifunction	A0A0N9HES5	Ras-related C3 botulinum toxin substrate 1 (*Mizuhopecten yessoensis*)	17	3	2	21.4	8.32	1.133	2.817
	K1PHM8	14-3-3 protein zeta (*Crassostrea gigas*)	6	3	2	28.6	4.93	1.432	4.084
	K1QIG6	ADP-ribosylation factor-like protein 3 (*Crassostrea gigas*)	10	3	3	28.2	9.20	0.885	8.223

MW = molecular weight; pI = isoelectric point; AR = abundance ratio